Japanese Journal of Applied Physics
Vol. 46, No. 4B, 2007, pp. 0000-0000

Transient Response in Monolithic Mach-Zehnder Optical Modulator Using (Ba,Sr)TiO_3 Film Sputtered at Low Temperature on Silicon

Masato SUZUKI, Kazuma NAGATA, Yuichiro TANUSHI and Shin YOKOYAMA

Research Center for Nanodevices and Systems, Hiroshima University, 1-4-2 Kagamiyama, Higashi-Hiroshima, Hiroshima 739-8527, Japan

(Received September 28, 2006; accepted for publication December 26, 2006; published online xxxx yy, zzzz))

We have fabricated Mach-Zhender interferometers (MZIs) using the (Ba,Sr)TiO_3 (BST) film sputter-deposited at 450°C, which is a critical temperature for the process after metallization. An optical modulation of about 10% is achieved when 200 V is applied (electric field in BST is $1.2x10^4$ V/cm). However, the response time of optical modulation to step function voltage is slow (1.0-6.3 s). We propose a model for the slow transient behavior based on movable ions and a long dielectric relaxation time for the BST film, and good qualitative agreement is obtained with experimental results.
[DOI: 10.1143/JJAP.46.dummy]

KEYWORDS: optical modulator, electro optic material, (Ba,Sr)TiO_3 (BST), Mach-Zhender interferometer, monolithic fabrication

1. Introduction

Recently, the switching speed of transistors has been improved and the performance of an LSI system is currently limited by the signal delay of global interconnections.[1] An optical intra chip interconnection instead of a conventional global metal interconnection has attracted considerable attention for improving the performance of LSIs further.[2] To realize optically interconnected LSIs, one method is to integrate many discrete light-emitting devices on an LSI by a bonding technique.[3] However, this technique is not suitable for mass production at the current stage. Therefore, we have proposed an optical interconnection system using optical switches made of electro optic (EO) material,[4,5] where external light is introduced into an LSI chip and an optical signal is modulated using the optical switches. This optical interconnection system should be monolithically integrated on the metallization layer to save the chip area.

(Ba,Sr)TiO_3 (BST) is one of the promising EO materials to be integrated on a Si substrate because a BST film was already used as a high-k dielectric film for memory capacitors in the research stage.[6] In our previous study, we have succeeded in operating a monolithic Mach-Zehnder interferometer (MZI) optical modulator on a Si substrate using a spin-coated BST film,[7] and found that it is necessary to anneal the spin-coated BST film at 550°C to produce a poly crystallized film. However, the temperature of 550°C is too high to fabricate optical switches after metallization process. The process temperature after metallization should not exceed 450°C.[8] In this study, we have succeeded in fabricating a monolithic MZI on a Si substrate using the BST film sputter-deposited at 450°C and evaluated the performance of the fabricated MZI. A model for the slow response of the MZI is also proposed

.

2. Experimental Procedure

BST films were deposited by RF magnetron sputtering. The structure of the RF magnetron sputtering machine used was reported in ref. 9 and the deposition condition is shown in Table I. Previously, it was reported that both the crystallinity and propagation loss of the BST films increase with growth temperature.[9] Although the BST film sputter-deposited at 450°C has a high crystallinity, the light propagation loss is very large (470 dB/cm).[9] Therefore, we fabricated the special structure shown in Fig. 1 in order to

Table I Conditions for sputtering of BST film.

RF power (W)	50
Base pressure (Pa)	1.2×10^{-6}
Sputtering gas	Ar=44 sccm, O_2 =11 sccm
Pressure (Pa)	2.0
Substrate temperature (°C)	450
Deposition rate (nm/min)	1.0

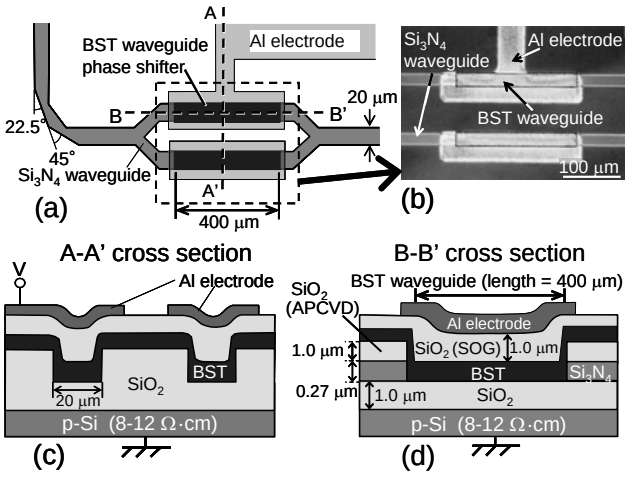

Fig. 1 (a) Schematic plan view, (b) photograph of the fabricated Mach-Zehnder interferometer, cross-sections along (c) A-A' and (d) B-B' in (a). In Fig. 1(b), a part of the bottom Al electrode is lacked for a poor resist process, but it does not affect the modulation of the MZI.

*Email address: yokoyama@sxsys.hiroshima-u.ac.jp

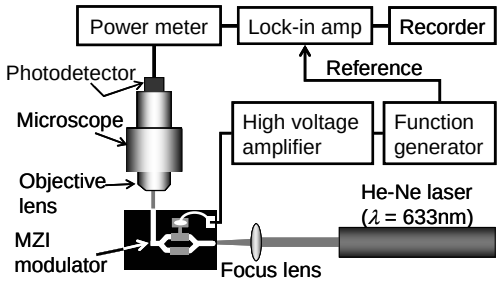

Fig. 2 Optical measurement system for MZI optical modulator. For quasi-static measurement, a power meter was directly connected to a recorder.

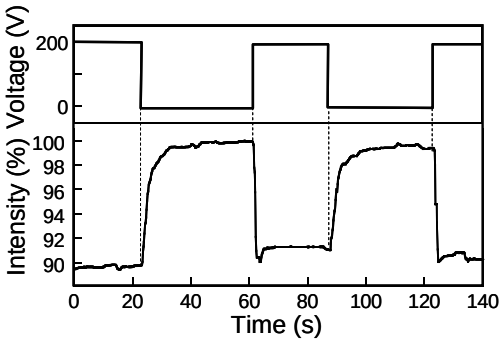

Fig. 3 Optical response of the BST MZI modulator when awith rectangular voltage was applied to one arm.

obtain both high crystallinity and small optical loss. In this structure, BST waveguides are used only as the phase shifters of the MZI and the other parts of the MZI are made of Si_3N_4 waveguides with a small propagation loss. For both BST and Si_3N_4 waveguides, the width is 20 μm and the thickness is 0.26 μm. The length of the BST phase shifters is 400 μm, and their optical loss is calculated to be 18.8 dB, which is still acceptable in an actual MZI. The light propagation loss of the Si_3N_4 waveguides is less than 5 dB/cm.[10)]

We fabricated the MZI by the following procedure. First, a Si_3N_4 film was deposited by low-pressure chemical vapor deposition (LPCVD) on a thermal SiO_2 layer (1.0 μm thick) and etched by reactive ion etching (RIE) in CF_4+H_2 to form Si_3N_4 waveguides. An SiO_2 layer (1.0 μm thick) was then deposited on the Si_3N_4 waveguides by atmospheric pressure CVD as an upper cladding layer for the Si_3N_4 waveguides. Parts of the Si_3N_4 waveguides and the upper cladding SiO_2 were etched by RIE to form BST waveguides, as shown in Fig. 1(d). Then, a BST film was deposited by RF magnetron sputtering at 450°C. A spin-on-glass (SOG: 1.0 μm thick) film was then deposited as an upper cladding layer for the BST waveguides. Finally, Al electrodes were formed by vacuum evaporation and wet etching.

Figure 2 shows an optical measurement system for the MZI optical modulator. He-Ne laser light (λ=633 nm) was introduced from the cleaved edge of the MZI, and the output light intensity was measured using a semiconductor photodetector (818-SL, Newport), an optical power meter (1830-C, Newport) and a lock-in amplifier (5600A, NF Electronic Instruments). The input light is transverse electric polarized. A voltage was applied to one arm of the MZI, and optical modulation characteristics were measured.

3. Results and Discussion

3.1 Voltage dependence of optical modulation

One example of the MZI response is shown in Fig. 3. The output intensity is changed by about 10 % at maximum when the applied voltage (V) is 200 V (BST layer electric field: E_{BST}= 1.2x10^4 V/cm). E_{BST} was calculated using a BST relative dielectric constant (ε_{BST}) of 330, which was

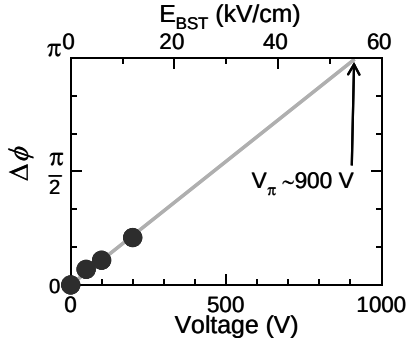

Fig. 4 Phase shift versus applied voltage of the MZI.

obtained by the quasi-static capacitance-voltage measurement of an Al/BST/SiO_2/Si capacitor. The voltage applied to p-type Si was estimated to be ~1 V because the inversion layer was formed with the stray light of the He-Ne laser. This result is higher than that of the MZI made of spin-coated and annealed (550°C) BST, for which the optical modulation was about 2% when E_{BST} = 1.3x10^4 V/cm.[7)] The reason for the high operation voltage of 200 V is that the voltage is mainly applied to two SiO_2 cladding layers with a small relative dielectric constant (ε_{sio2}=3.9) and the electric field in the BST layer with a larger dielectric decreases.

Figure 4 shows the voltage dependence of the phase shift ($\Delta\phi$) of the MZI, where $\Delta\phi$ is given by [11)]

$$I = I_0 \frac{1+\cos(\Delta\phi)}{2} \quad . \qquad (1)$$

Here, I is the output intensity and I_0 is the maximum output intensity of the MZI. The optical phase shift $\Delta\phi$ is proportional to the applied voltage, as shown in Fig. 4, suggesting that the light is modulated by the EO effect of the BST phase shifters in the MZI. V_π=900 V and $V_\pi L$=36 V·cm are estimated by extrapolating of the measured phase shift shown in Fig. 4, where V_π is the drive voltage required for the phase shift π and L is the length of the BST phase shifters (L=400 μm). These results are higher than those of an MZI made of crystal $LiNbO_3$ (V_π=6 V and $V_\pi L$=3 V·cm).[12)] The low performance of our MZI is

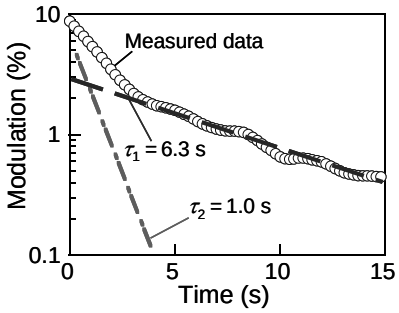

Fig. 5 Deconvolution of different time constants in the time region between 87 s and 102 s in Fig. 3.

caused by the insufficient crystallinity of the BST film and an unoptimized device design.

3.2 Transient analysis and mechanism of MZI

In Fig. 3, when the voltage is switched from 0 to 200 V (t=60 s), the output rapidly decreases and then slowly slightly increases with a time constant of τ_0~2 s. On the other hand, when the voltage is changed from 200 to 0 V (t=87 s), the output increases slowly. The time constant of this output increase is analyzed in Fig. 5, and the two time constants τ_1=6.3 s and τ_2=1.0 s are obtained.

As the reason for the slow optical modulation, the resistance-capacitance (RC) delay time of the Al electrode and Al/SiO_2/BST/SiO_2/Si capacitor is very short (about 1.2 ps). The heating effect generated by the leakage current is also negligible, as indicated in the following order estimation. The leakage current is very small (about 1.3×10^{-7} A/cm^2 at V=200 V) owing the thick SiO_2 cladding layers. The temperature increase at a steady state is simply estimated using a one-dimensional model, and also the thermal conductivity of the Si substrate is assumed to be the same as that of SiO_2 for simplifying the calculation. As a result, the temperature increase of the BST layer is in the order of 10^{-5} °C at maximum. Then, the optical modulation due to the heating effect generated by the leakage current is roughly estimated to be in the order of 10^{-4}, which is negligible compared with the measured modulation (0.1). Here, we used the thermo optic coefficient of the $LiNbO_3$ crystal [13] for this estimation because that of the BST film has not yet been reported.

Therefore, we considered that the transient behavior of the optical modulation may be caused by the electric and optical properties of the BST film. The model of the transient behavior of the MZI is proposed in Fig. 6: (a) cross section, (b) output intensity versus E_{BST}, (c) output intensity with time, and (d) dielectric relaxation characteristics of the BST film. In Fig. 6(b), the E_{BST} dependence of the output intensity is indicated, which is given by eq. (1), where $\Delta\phi$ is proportional to E_{BST}, as shown in Fig. 4. The dielectric relaxation characteristics of the BST film are schematically shown in Fig. 6(d).[14, 15] We assumed that there are some movable ions in the BST film

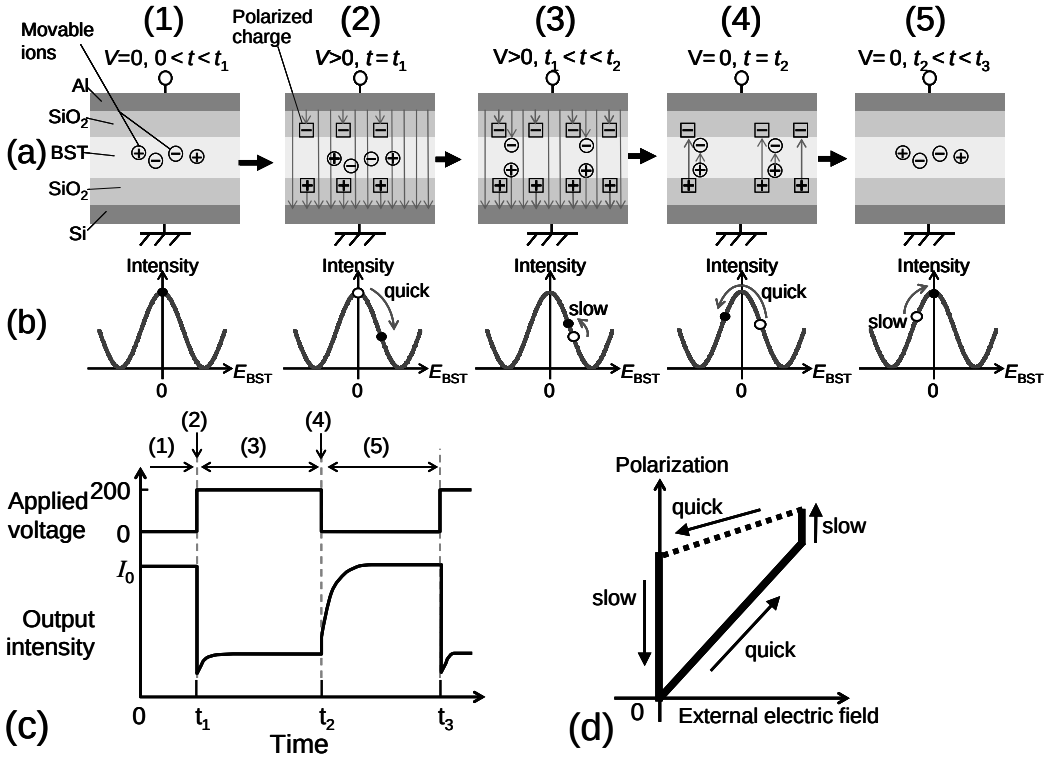

Fig. 6 Model of MZI transient behavior of MZI. (a) Cross- section of the MZI, where arrows indicate electric field. (b) Output intensity versus electric filed in BST. (c) Optical response based on the proposed model. (d) Dielectric polarization characteristics of the BST film. The BST film used in this study is $(Ba_{0.35},Sr_{0.37})TiO_{3.07}$.

because it is not perfectly stoichiometric.[16] (1) At the initial state (V=0, $0<t<t_1$), there is no electric field in the BST layer and the output intensity is maximum. (2) When the voltage is applied (V>0, $t=t_1$), an electric filed is generated and polarized charges are rapidly induced at the SiO_2/BST interface, resulting in a rapid decay at the output intensity. (3) Subsequently movable ions slowly drift toward the BST/SiO_2 interface owing to the electric field in the BST layer. Also, additional interface charges are induced by the slow dielectric relaxation effect of the BST film.[14,15] These charges reduce the electric field in the BST layer. Therefore, the output intensity slowly slightly increases. The time constant τ_0~2 s (discussed in the first paragraph in this section) may correspond to the time constants of the ion drift and dielectric relaxation effect. (4) When the voltage is switched to 0 V ($t=t_2$), the external electric field is removed. However, the movable ions remain at the BST/SiO_2 interface and some polarized charges do not disappear immediately, as shown in Fig. 6(d), owing to the slow dielectric relaxation effect.[14,15] These charges generate an electric field in the opposite direction in the BST layer compared with that immediately before voltage switching (Fig. 6(b), (3)). As a result, the output intensity does not rapidly return to its initial maximum value but rapidly slightly increases at $t=t_2$ [Fig. 6(b), (4)]. (5) Then, the output intensity slowly increases to the initial state with decreasing the interface charge density. The measured time constants τ_1=6.3 s and τ_2=1.0 s may correspond to the time constants of the ion drift and dielectric relaxation effect. However, it is unclarified to which phenomenon these time constants belong at this stage.

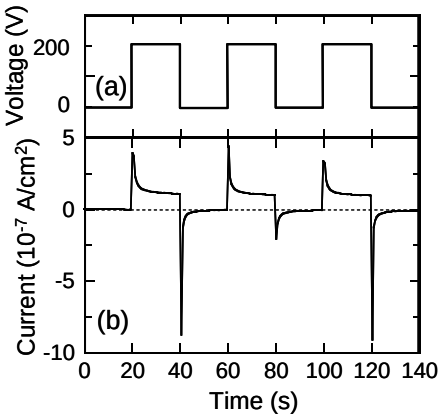

Fig. 7 Time dependences of (a) applied voltage and (b) measured current between Al electrode and Si substrate of the MZI. The large scattering of the observed peak current height may be attributed to the asynchronized sampling time of the current meter to the applied voltage.

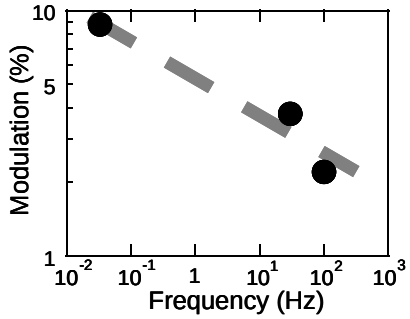

Fig. 8 Frequency dependence of the BST MZI optical modulation

Figure 7 shows the time dependence of the measured current between the Al electrode and the Si substrate with an applied rectangular voltage waveform. When the applied voltage is changed from 0 to 200 V or from 200 to 0 V, the sharp peak current flows owing to the rapid polarization of the BST and SiO_2 films. Additionally, the slow current decay follows the peak current, which may be induced by the slow dielectric relaxation effect and/or movable ions. This result supports the above-mentioned transient mode based on the dielectric relaxation effect and movable ions. The leakage current of about 2×10^{-7} A/cm^2 flows when a voltage of 200V is applied, because SOG is not highly insulative, for which the measured conductivity is about 10^{12} Ω·cm.

Here, the origin of the movable ions is discussed. In a stoichiometric BST, the ratio of Ba+Sr : Ti : O is 1 : 1 : 3. However, the Ba+Sr : Ti : O ratio of the BST film used in this study was evaluated to be 1 : 1.39 : 4.26 by X-ray photoelectron spectroscopy measurement. Therefore, excess Ti^{4+} and O^{2-} ions may act as positive and negative movable ions, respectively.

Figure 8 indicates the frequency dependence of the modulation. The modulation decreases with an increase in frequency. From the limitation of the response time of the power meter, the maximum measured frequency is 100 Hz in this study. The slow response components discussed above must have led to the large frequency dependence.

3.3 Optical mode in multimode MZI

Here, it is necessary to note that the waveguides used for the MZI are wider than a single-mode waveguide. As a result, the output light intensity of the MZI is sufficiently high, resulting in the observation of the optical modulation. However, the light propagation mode becomes multimode. From the simulation, there are 92 modes in the width direction of the BST waveguide. Rivlin *et al.* reported that the interference in a multimode MZI with a large number of modes is very complex and the optical modulation by such interference is zero mathematical expectation.[17] Nevertheless, Fig. 4 indicates that the MZI in this study acts similarly to a single-mode MZI. At this stage, there is no absolutely convincing explanation for the single-mode-like operation of the fabricated MZI. However, we assumed the following reason for this phenomenon. That is, only the fundamental mode and several modes near the fundamental mode may dominate the output light. As shown in Fig. 1(d), the BST phase shifters are not completely defined; however, they are connected to the outer part of the waveguide region through steps of 1.27 μm height. As a result, some propagating light leaks when it reflects at the sidewall of the BST waveguide. Figures

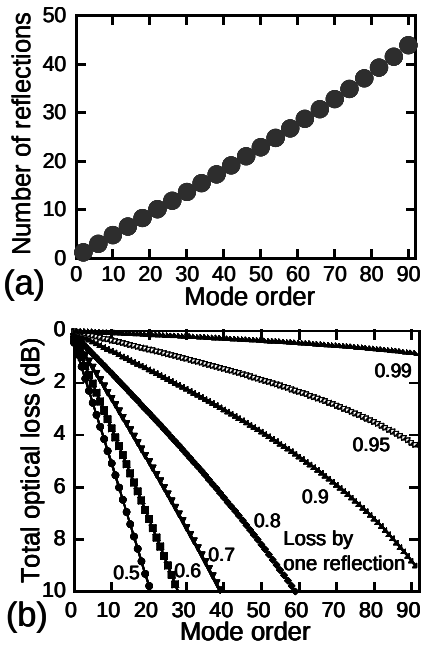

Fig. 9 (a) Number of propagating light reflections of the propagating light versus mode order. (b) Total optical loss versus mode order of propagating modes generated by reflection. Here, a the propagation angle of each mode was calculated from an equivalent index, and then the number of reflections was analytically calculated using the propagation angle.

9(a) and 9(b) show the calculated number of propagating light reflections at the sidewall and total leakage loss versus mode order, respectively. Higher order modes are more rapidly diminished because of a large number of reflections. On the other hand, the fundamental mode and several modes near the fundamental mode slowly decay and may dominate the output light. From this mechanism, although the MZI is multimode, it may work similarly to a single-mode MZI.

To improve the performance of the BST MZI, it is necessary to fabricate a single-mode BST waveguide where both high crystallinity and low propagation loss are achieved. We have pointed out that that the light scattering induced by poly crystalline grains is the major cause of the BST waveguide propagation loss.[9] Therefore, the propagation loss may be reduced by aligning the direction of the BST grains. Graphoepitaxy, in which an artificial surface topographic pattern can control the orientation of crystal grains,[18] is one possible method of improving the optical properties of the BST waveguide. Additionally, the crystal quality of BST in the thickness direction may be improved by inserting a buffer layer, e.g., MgO [19] between a SiO_2 cladding layer and a BST layer.

4. Summary

We have, for the first time, succeeded in operating an MZI modulator made of a BST film deposited at 450°C on a Si substrate and achieved a modulation of about 10%. The transient response and frequency dependence of the MZI were investigated, and a model of the observed slow transient behavior was proposed on the basis of the movable ions and slow dielectric relaxation of a nonstoichiometric BST film. The reason for the successful operation even for a multimode MZI was also determined. An improvement in BST film quality is essential for obtaining a higher MZI performance. The operation voltage is expected to be reduced using a suitable device design.

Acknowledgments

This study was supported in part by the 21st Century COE program "Nanoelectronics for Tera-Bit Information Processing," and a Grant-in-Aid for Scientific Research (B) (No. 17360166) both from the Ministry of Education, Culture, Sports, Science and Technology of Japan.

1) J.A. Davis, V.K. De, James and D. Meindl: IEEE Trans. Electron Devices **45** (1998) 580.
2) I. Hayashi: Jpn. J. Appl. Phys. **32** (1993) 266.
3) Y. Sasaki, T. Katayama, T. Koishi, K. Shibahara, S. Yokoyama, S. Miyazaki and M. Hirose, J. Electrochem. Soc. **146** (1999) 710.
4) Y. Tanushi M. Wake, K. Wakushima, M. Suzuki and S. Yokoyama: 1st Int. Conf. Group IV Photonics, Hong Kong, 2004, WB3.
5) Y. Tanushi and S. Yokoyamae: Jpn. J. Appl. Phys. **45** (2006) 3493.
6) K Ohashi, J. Fujikata, M. Nakada, T. Ishi, K. Nishi, H. Yamada, M. Fukaishi, M. Mizuno, K. Nose, I. Ogura, Y. Urino and T. Baba: [IEEE IEDM Tech. Dig., New York], 1996, p. 675.
7) Z. M. Xu, M. Suzuki, Y. Tanushi and S. Yokoyama, Appl. Phys. Lett. **88** (2006) 161107.
8) M. Salib, M. Morse and M. Paniccia: 1st Int. Conf. Group IV Photonics, Hong Kong, 2004, PLE1.
9) M. Suzuki, Z.M. Xu, Y. Tanushi and S. Yokoyama: Jpn. J. Appl. Phys. **45** (2006) 3488.
10) T. Nagata, T. Tanaka, K. Miyake, H. Kurotaki, S. Yokoyama and M. Koyanagi: Jpn. J. Appl. Phys. **33** (1994) 822.
11) H. Nishihara, M. Haruna and T. Suhara: *Optical Integrated Circuits* (McGraw-Hill, New York, 1989) p. 286.
12) T. R. Ranganath and S. Wang: IEEE J. Quantum Electron **13** (1977) 290.
13) G. Ghosh: Opt. Lett. **19** (1994) 1391.
14) H. Matsuura: Jpn. J. Appl. Phys. **36** (1997) 3569.
15) T. Horikawa, T. Makita, T. Kuroiwa and N. Mikami: Jpn. J. Appl. Phys. **34** (1995) 5478.
16) T. Kikkawa, N. Fujiwara, H. Yamada and S. Miyazaki: Appl. Phys. Lett. **81** (2002) 2821.
17) L. A. Rivlin, A. T. Semenov and N. V. Shelkov: Sov. J. Quantum Electron. **15** (1985) 128.
18) H. I. Smith and D. C. Flanders: Appl. Phys. Lett. **32** (1978) 349.
19) N. A. Basit, H. K. Kima and J. Blachere: Appl. Phys. Lett. **73** (1998) 3491.